Egypt. J. Chem. **Vol. 67**, No. 12 pp. 111 - 127 (2024)

Egyptian Journal of Chemistry

http://ejchem.journals.ekb.eg/

Discovery of Novel *N*-Acetylpyrazolines as Microtubule Inhibitors: Design, Synthesis, Anticancer Evaluation, and Molecular Docking Study

Islam H. Ali[a], Ahmed M. El Kerdawy[b,c], Rasha Z. Batran[d], Rasha M. Allam[e], Mahmoud T. Abo-elfadl[f,g], Francesca Sciandra[h], Iman A. Y. Ghannam[a,*]

[a]*Chemistry of Natural and Microbial Products Department, Pharmaceutical and Drug Industries Research Institute, National Research Centre, Dokki, Cairo 12622, Egypt.*

[b]*School of Pharmacy, College of Health and Science, University of Lincoln, Joseph Banks Laboratories, Green Lane, Lincoln, United Kingdom*

[c]*Department of Pharmaceutical Chemistry, Faculty of Pharmacy, Cairo University, Cairo 11562, Egypt.*

[d]*Chemistry of Natural Compounds Department, Pharmaceutical and Drug Industries Research Institute, National Research Centre, Dokki, Cairo 12622, Egypt.*

[e]*Pharmacology Department, Medical Research and Clinical Studies Institute, National Research Centre, Dokki, Cairo 12622, Egypt.*

[f]*Cancer Biology and Genetics Laboratory, Centre of Excellence for Advanced Sciences, National Research Centre, Dokki, 12622 Cairo, Egypt.*

[g]*Biochemistry Department, Biotechnology Research Institute, National Research Centre, Dokki, Cairo, Egypt.*

[h]*Istituto di Scienze e Tecnologie Chimiche "Giulio Natta"- SCITEC (CNR) Sede di Roma, Largo F. Vito 1, 00168 Roma, Italy.*

Abstract

In the current study, a new series of *N*-acetylpyrazolines (**6a-d**) were designed and synthesized from their corresponding chalcones and hydrazine hydrate in acidic medium. The *N*-acetylpyrazolines (**6a-d**) were tested for their anti-hepatocellular activity against liver cancer (HuH-7, and HepG-2), and normal BNL cell lines and compared with paclitaxel, colchicine, and combrestatin A-4 (CA-4), as standards, and their IC_{50} values were determined. The 3',4',5'-trimethoxyphenyl *N*-acetylpyrazoline derivative **6d** was the found the most potent *N*-acetylpyrazoline derivative IC_{50} = 0.30, and 77.30 µM, respectively, and found non-cytotoxic to the normal BNL cell line. While compounds **6b**, and **6c** revealed lower anticancer activity against HuH-7 cell line IC_{50} = 14.50, and 11.00 µM, respectively. Moreover, the *N*-acetylpyrazolines **6a-d** were evaluated for their anticancer screening against different cancer cell lines at 10 µM by the Developmental Therapeutic Program (DTP) - NCI - USA, and they showed mean GI% ranges 8.87-64.54%. The 3',4',5'-trimethoxyphenyl *N*-acetylpyrazolines **6c**, and **6d** revealed potent anticancer activities and lethal effects against lung cancer cell line (HOP-92) for **6c** and melanoma cell line (SK-MEL-5) for **6d** with GI% values of 104.80, and 109.52%, respectively. Furthermore, the *N*-acetylpyrazolines **6a-d** enhanced tublin polymerization, and showed tubulin-stabilizing effects as paclitaxel at 50 µM. A molecular docking study was performed for the *N*-acetylpyrazolines **6a-d** to investigate the binding pattern at the Taxol-binding site of microtubules. A physicochemical prediction and ADME properties as well as drug-likeness and medicinal chemistry friendliness of compounds **6a-d** were also performed.

Keywords: *N*-acetylpyrazolines; Tubulin polymerization inhibitors; Anticancer activity; Molecular docking study

*Corresponding author e-mail: iman.youssef.ghannam@gmail.com, ia.ghannam@nrc.sci.eg (I. A. Y. Ghannam)
EJCHEM use only: Received date 08 May 2024; revised date 25 June 2024; accepted date 01 July 2024
DOI: 10.21608/EJCHEM.2024.288226.9691

1. Introduction

Cancer is the most serious life-threatening disease, and one of the leading causes of global mortality [1, 2]. Liver cancer is considered as one of the global health challenges and its incidence is increasing worldwide [3], and it is estimated that more than one million individuals will be affected annually by liver cancer by 2025 [4]. Eighty percent of instances of liver cancer are attributed to hepatocellular carcinoma (HCC), which is the most common type of liver cancer [5]. Tubulin is one of the molecular targets for antitumor agents *via* targeting the dynamic process of microtubules assembly, and disassembly which can be hindered through various targeting agents that can bind to different sites in the β-tubulin subunit [6]. The microtubule targeting agents, Interference with the microtubule function, can do cellular arrest at G2/M phase, hence, leading to cell death through both induction of apoptosis and necrosis [7, 8]. The structural elements of the mitotic spindle are microtubules, which are hollow cylindrical filaments that are assembled by the aggregation of α- and β-tubulin heterodimers [9]. Numerous biological activities, such as intracellular trafficking, the formation of the cell skeleton, cell migration, and cell division, depend critically on microtubules [10, 11]. Paclitaxel (**I**), and colchicine (**II**) are naturally occurring microtubules targeting agents at distinctive binding sites (Figure 1), and act as a microtubule stabilizing and destabilizing agent, respectively [12]. The microtubule stabilizing agents bind to taxane site that can accelerate microtubule assembly; paclitaxel (**I**), have been successfully applied in tumor therapy, and some microtubule stabilizing agents have entered also in clinical studies [13, 14]. However, these tubulin targeting agents have various drawbacks; poor pharmacokinetic properties, high lipophilicity, low water solubility, and multi-drug resistance [15, 16]. Pyrazoline containing compounds, privileged scaffold found in many biologically active agents, that are characterized with diversity in their biological activities including anticancer activity [17-23]. Pyrazolines act as anticancer agents *via* different mechanisms including; tyrosine kinase inhibitors [24-28], and tubulin suppressors [29-32]. The *N*-methylindole-pyrazoline hybrids (**IIIa-c**) (Figure 2) showed tubulin polymerization inhibition and anticancer activities [33], whereas, the 3',4',5'trimethoxyphenyl *N*-methylindole-pyrazoline hybrid (**IIIa**) revealed tubulin inhibition IC_{50} = 2.12 µM, and potent anticancer activity against diverse cancer cell lines; HepG2, HeLa, MCF-7, and A549 with IC_{50} values 0.31, 0.21, 0.29, and 0.26 µM, respectively [34]. The 3-methoxyphenyl *N*-methylindole-pyrazoline hybrid (**IIIb**) (YMR-65) showed relatively similar tubulin polymerization inhibition as compound (**IIIa**), IC_{50} = 2.44 µM, and high anticancer activity IC_{50} = 0.31, 0.25, 0.32, and 0.28 against HepG2, HeLa, MCF-7, A549 cancer cell lines, respectively [33, 35]. Furthermore, it demonstrated potent *in vivo* anticancer efficacy, and low toxicity in pharmacokinetic and pharmacodynamics studies [36]. Later, the *N*-nicotinoylpyrazoline derivative (**IIIc**) was developed for better stability, and less susceptibility to metabolism [37]. Moreover, it displayed more potent tubulin inhibition IC_{50} = 1.60 µM, and potent anticancer activity GI_{50} ranges 0.09-0.59 µM against HepG2, HeLa, A-549, and MCF-7 cancer cell lines. An *in vivo* study was also performed and demonstrated a comparable anticancer activity to combrestatin A-4 (CA-4) in HeLa-xenograft mice model without tissue damage, and weight loss [37]. Besides, the *N*-phenylpyrazole derivative (**IVa**) showed anticancer activity against the colon cancer cell line HCT-116 (IC_{50} = 2.65 µM), and tubulin polymerization inhibition IC_{50} = 10.9 µM, as well as induction of cell cycle arrest in HCT-116 cancer cell line at G2/M phase. *in vivo* study for this pyrazole derivative (**IVa**) showed effect in decreasing tumor growth in a HCT-116 mouse model and showed no toxicity [38]. In contrast, the *N*-phenylpyrazole derivative (**IVb**) caused cell cycle arrest in G2/M phase and interfered with the production of mitotic spindles in MCF-7 cells, demonstrating strong anticancer activity against the cancer cell lines B16F10, Hela, and MCF-7 (IC_{50} = 1.3, 6.0, and 5.5 µM, respectively) (Figure 2) [30]. The indole-pyrazole hybrid (**V**) showed potent anticancer activity against the hepatocellular cancer cell (HCC) lines; HuH-7, HepG-2, Mahlavu, and SNU475 with IC_{50} range 0.6-2.9 µM, and showed moderate inhibitory activity against tubulin polymerization (IC_{50} = 19 µM). It also induced cell cycle arrest at the G2/M phase in HuH-7 and Mahlavu cell lines, as well as induction of apoptosis in HCC cells (Figure 2) [32].

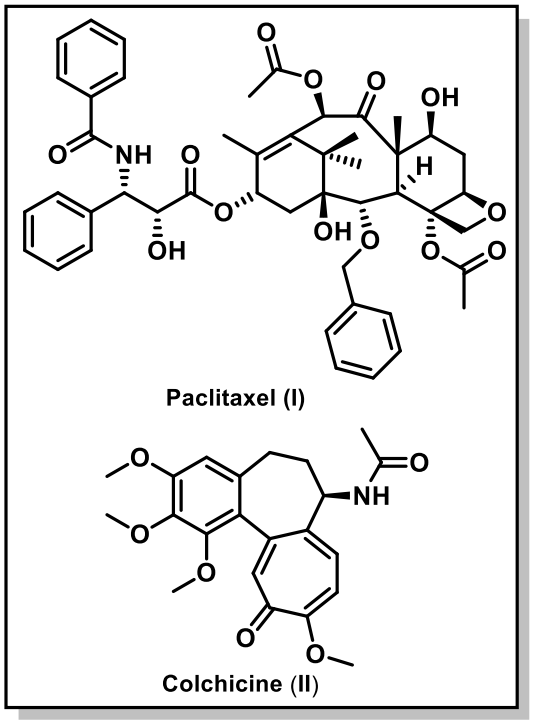

Figure 1: Chemical structures of some naturally occurring tubulin polymerization inhibitors: paclitaxel (**I**), and colchicine (**II**).

Based on the above mentioned findings, a series of novel *N*-acetylpyrazolines **6a-d** were designed, synthesized from the corresponding chalcones, and evaluated *in vitro* for their anticancer activity against liver cancer and normal (BNL) cell lines, as well as anticancer screening against a panel of cancer cell lines at 10 µM. This was coupled with tubulin polymerization assay for the synthesized *N*-acetylpyrazolines. To investigate the binding pattern of the synthesized compounds, a molecular docking study was also performed for the *N*-acetylpyrazolines to at the paclitaxel-binding site of microtubules *via* key amino acids.

2. Experimental

2.1. Chemistry:

The measured melting points were determined using a Daihan Melting Point Analyzer, and were uncorrected. A 400 (100) MHz Bruker Spectrometer at the Microanalytical Unit, Faculty of Pharmacy, Cairo University, Egypt, was used to report the NMR spectra. An Advion compact mass spectrometer (CMS) at Nawah Scientific in Cairo, Egypt, was used to report mass spectra (MS-ESI).

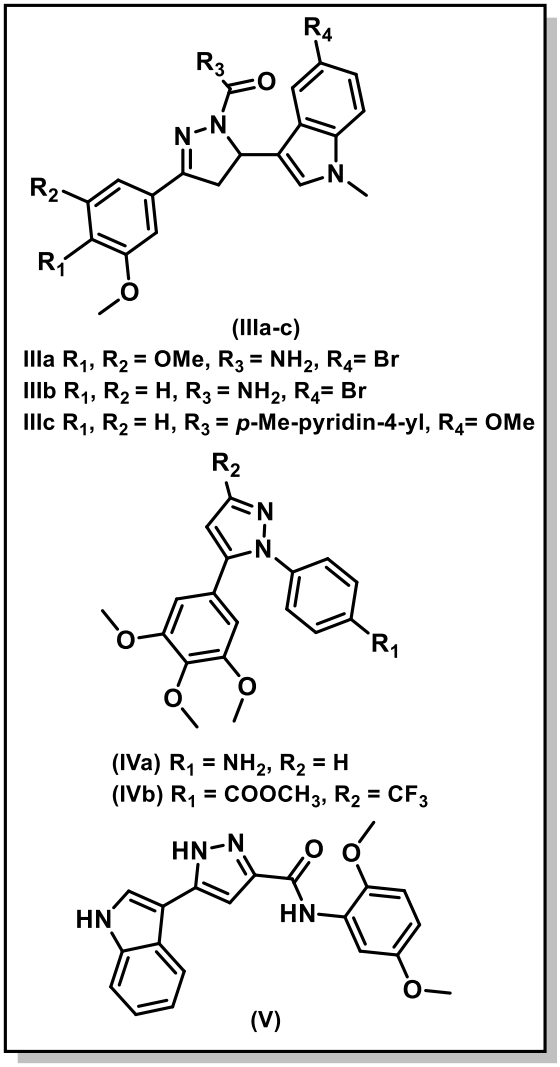

Figure 2: Chemical structures of some reported pyrazolines (**IIIa-c**), and pyrazoles (**IV, V**) as tubulin polymerization inhibitors

2.1.1. General procedure for the synthesis of chalcones 5a-d

To a stirred solution of the appropriate 4-(benzyloxy)-3-methoxybenzaldehyde **3a-c** (5 mmol) and 3',4'-dimethoxyacetophenone **4a** or 3',4',5'-trimethoxyacetophenone **4b** (5 mmol) in MeOH (40 ml) was added 50% aqueous KOH (15 ml) and heated under reflux with stirring for 1-4 h. The solvent was evaporated and the precipitate was formed, filtered, evaporated and purified either by recrystallization from absolute ethanol or by column chromatography ethyl acetate: petroleum ether (60-80 °C) (1:1).

2.1.1.1. (*E*)-3-(4-(Benzyloxy)-3-methoxyphenyl)-1-(3,4-dimethoxyphenyl)prop-2-en-1-one (**5a**)

Yellow solid; Yield (80%); mp 173-174 °C; IR (KBr) υ_{max}: 3062, 1661 cm^{-1}; ^{1}H NMR (400 MHz, DMSO-d_6) δ: 3.85 (s, 3H, OCH_3), 3.87 (s, 6H, 2 OCH_3), 5.16 (s, 2H, OCH_2), 7.10 (dd, *J* = 2.4 Hz, *J* = 8.4 Hz, 2H, H_{ar}), 7.30-7.42 (m, 4H, H_{ar}), 7.46 (d, *J* = 8.0 Hz, 2H, H_{ar}), 7.54 (s, 1H, H_{ar}), 7.60 (s, 1H, H_{ar}), 7.67 (d, *J* = 12.0 Hz, 1H, CH=C<u>H</u>-CO), 7.83 (d, *J* = 16.0 Hz, 1H, C<u>H</u>=CH-CO), 7.92 (d, *J* = 8.0 Hz, 1H, H_{ar}) ppm; ^{13}C NMR (100 MHz, DMSO-d_6) δ: 55.63 (OCH_3), 55.82 (OCH_3), 55.97 (OCH_3), 69.89 (OCH_2), 110.73 (CH_{ar}), 110.83 (CH_{ar}), 111.39 (CH_{ar}), 113.18 (CH_{ar}), 119.77 (CH_{ar}), 123.41 (CH=<u>C</u>H-CO), 127.96, (CH_{ar}), 128.03 (C_{ar}), 128.05 (CH_{ar}), 128.53 (CH_{ar}), 130.82 (CH_{ar}), 136.81 (C_{ar}), 143.59 (<u>C</u>H=CH-CO), 148.87 (C_{ar}), 149.34 (C_{ar}), 150.11 (C_{ar}), 154.16 (C_{ar}), 187.40 (C=O) ppm; MS (ESI^+, m/z): 427.1 (89.6%) $[M + Na]^+$; Anal. Calcd for $C_{25}H_{24}O_5$: C, 74.24; H, 5.98; Found: C, 74.33; H, 6.11.

2.1.1.2. (*E*)-3-(4-(4-Fluorobenzyloxy)-3-methoxyphenyl)-1-(3,4-dimethoxyphenyl)prop-2-en-1-one (**5b**)

Yellow solid; Yield (86%); mp 135-136 °C; IR (KBr) υ_{max}: 3068, 1665 cm^{-1}; ^{1}H NMR (400 MHz, DMSO-d_6) δ: 3.86 (s, 3H, OCH_3), 3.87 (s, 6H, 2 OCH_3), 5.14 (s, 2H, OCH_2), 7.10 (dd, *J* = 3.2 Hz, *J* = 8.4 Hz, 2H, H_{ar}), 7.23 (t, *J* = 8.4 Hz, 2H, H_{ar}), 7.40 (d, *J* = 8.0 Hz, 1H, H_{ar}), 7.49-7.55 (m, 3H, H_{ar}), 7.60 (s, 1H, H_{ar}), 7.68 (d, *J* = 15.6 Hz, 1H, CH=C<u>H</u>-CO), 7.84 (d, *J* = 15.6 Hz, 1H, C<u>H</u>=CH-CO), 7.93 (d, *J* = 8.4 Hz, 1H, H_{ar}) ppm; ^{13}C NMR (100 MHz, DMSO-d_6) δ: 55.58 (OCH_3), 55.77 (OCH_3), 55.82 (OCH_3), 69.12 (OCH_2), 110.70 (CH_{ar}), 110.78 (CH_{ar}), 111.40 (CH_{ar}), 113.21 (CH_{ar}), 115.18 (d, $^2J_{CF}$ = 22.0 Hz, <u>C</u>H_{ar}-C_{ar}F), 119.78 (CH=<u>C</u>H-CO), 123.32 (CH_{ar}), 128.07 (C_{ar}), 130.11 (d, $^3J_{CF}$ = 8.0 Hz, <u>C</u>H_{ar}-CH_{ar}-C_{ar}F), 130.77 (CH_{ar}), 133.00 (CH_{ar}), 133.03 (C_{ar}), 143.47 (<u>C</u>H=CH-CO), 148.81 (C_{ar}), 149.29 (C_{ar}), 149.92 (C_{ar}), 153.10 (C_{ar}), 160.65 (d, $^1J_{CF}$ = 242.0 Hz, C_{ar}-F), 187.30 (C=O) ppm; MS (ESI^+, m/z): 445.1 (79.8%) $[M + Na]^+$; Anal. Calcd for $C_{25}H_{23}FO_5$: C, 71.08; H, 5.49; Found: C, 71.23; H, 5.56.

2.1.1.3. (*E*)-3-(4-(Benzyloxy)-3-methoxyphenyl)-1-(3,4,5-trimethoxyphenyl)prop-2-en-1-one (**5c**)

Yellow solid; Yield (88%); mp 128 °C; IR (KBr) υ_{max}: 3063, 1651 cm^{-1}; ^{1}H NMR (400 MHz, DMSO-d_6) δ: 3.77 (s, 3H, OCH_3), 3.87 (s, 3H, OCH_3), 3.90 (s, 6H, 2 OCH_3), 5.17 (s, 2H, OCH_2), 7.11 (d, *J* = 8.4 Hz, 1H, H_{ar}), 7.32-7.36 (m, 1H, H_{ar}), 7.38-7.42 (m, 4H, H_{ar}), 7.43-7.47 (m, 3H, H_{ar}), 7.53 (s, 1H, H_{ar}), 7.71 (d, *J* = 15.2 Hz, 1H, CH=C<u>H</u>-CO), 7.80 (d, *J* = 15.6 Hz, 1H, C<u>H</u>=CH-CO) ppm; ^{13}C NMR (100 MHz, DMSO-d_6) δ: 55.88 (OCH_3), 56.25 (OCH_3), 60.20 (OCH_3), 69.85 (OCH_2), 106.21 (CH_{ar}), 112.07 (CH_{ar}), 113.25 (CH_{ar}), 119.85 (CH_{ar}), 123.20 (CH=<u>C</u>H-CO), 127.86 (CH_{ar}), 127.96 (C_{ar}), 128.46 (CH_{ar}), 133.31 (C_{ar}), 136.76 (C_{ar}), 141.87 (C_{ar}), 144.27 (<u>C</u>H=CH-CO), 149.26 (C_{ar}), 150.19 (C_{ar}), 152.90 (C_{ar}), 187.93 (C=O) ppm; Anal. Calcd for $C_{26}H_{26}O_6$: C, 71.87; H, 6.03; Found: C, 71.93; H, 6.14.

2.1.1.4. (*E*)-3-(4-(4-Methylbenzyloxy)-3-methoxyphenyl)-1-(3,4,5-trimethoxyphenyl)prop-2-en-1-one (**5d**)

Yellow solid; Yield (84%); mp 103 °C; IR (KBr) υ_{max}: 3078, 1651 cm^{-1}; ^{1}H NMR (400 MHz, DMSO-d_6) δ: 2.30 (s, 3H, CH_3), 3.76 (s, 3H, OCH_3), 3.85 (s, 3H, OCH_3), 3.89 (s, 6H, 2 OCH_3), 5.10 (s, 2H, OCH_2), 7.09 (d, *J* = 8.4 Hz, 1H, H_{ar}), 7.19 (d, *J* = 8.0 Hz, 2H, H_{ar}), 7.33 (d, *J* = 7.6 Hz, 2H, H_{ar}), 7.40-7.43 (m, 3H, H_{ar}), 7.51 (s, 1H, H_{ar}), 7.69 (d, *J* = 15.6 Hz, 1H, CH=C<u>H</u>-CO), 7.79 (d, *J* = 15.6 Hz, 1H, C<u>H</u>=CH-CO) ppm; ^{13}C NMR (100 MHz, DMSO-d_6) δ: 20.90 (CH_3), 55.99 (OCH_3), 56.37 (OCH_3), 60.36 (OCH_3), 69.89 (OCH_2), 106.30 (CH_{ar}), 112.03 (CH_{ar}), 113.37 (CH_{ar}), 119.88 (CH_{ar}), 123.45 (CH=<u>C</u>H-CO), 127.89 (C_{ar}), 128.12 (CH_{ar}), 129.16 (CH_{ar}), 133.45 (C_{ar}), 133.80 (C_{ar}), 137.43 (C_{ar}), 141.99 (C_{ar}), 144.51 (<u>C</u>H=CH-CO), 149.40 (C_{ar}), 150.37 (C_{ar}), 153.03 (C_{ar}), 188.16 (C=O) ppm; Anal. Calcd for $C_{27}H_{28}O_6$: C, 72.30; H, 6.29; Found: C, 72.41; H, 6.38.

2.1.2. General procedure for the synthesis of 1-acetyl-4,5-dihydropyrazoles 6a-d

To a solution of 15 mL of glacial acetic acid, (0.016 mol) of 80% hydrazine hydrate, (0.004 mol) of previously synthesized chalcones **5a-d** in absolute ethanol was added and the mixture was stirred and heated under reflux for 2-5 h, the solid precipitated and was filtered and dried. The crude product was purified using column chromatography. The eluent was ethyl acetate: petroleum ether (60-80 °C) (2: 3).

2.1.2.1. 1-(5-(4-(Benzyloxy)-3-methoxyphenyl)-4,5-dihydro-3-(3,4-dimethoxyphenyl)pyrazol-1-yl) ethanone (**6a**)

Off-white crystals; Yield (69%); mp 132-133 °C; IR (KBr) υ_{max}: 3074, 2928, 1651 cm^{-1}; ^{1}H NMR (400 MHz, DMSO-d_6) δ: 2.30 (s, 3H, CO-CH_3), 3.14 (dd, *J* = 4.0 Hz, *J* = 12.0 Hz, 1H, $H_{pyrazoline}$), 3.75 (s, 3H, OCH_3), 3.76-3.78 (m, 1H, $H_{pyrazoline}$), 3.80 (s, 3H, OCH_3), 3.81 (s, 3H, OCH_3), 5.04 (s, 2H, OCH_2), 5.47 (dd, *J* = 4.0 Hz, *J* = 8.0 Hz, 1H, $H_{pyrazoline}$), 6.62 (1H, d, *J* = 8.0 Hz, H_{ar}), 6.83 (s, 1H, H_{ar}), 6.95 (d, *J* = 8.0 Hz, 1H, H_{ar}), 7.01 (d, *J* = 8.4 Hz, 1H, H_{ar}), 7.27-7.33 (m, 2H, H_{ar}), 7.36-7.43 (m, 5H, H_{ar}) ppm; ^{13}C NMR (100 MHz, DMSO-d_6) δ: 21.80 (CO-$\underline{C}H_3$), 42.30 ($CH_{Pyrazoline}$), 55.56 (OCH_3), 55.62 (OCH_3), 55.64 (OCH_3), 59.11 ($CH_{Pyrazoline}$), 70.00 (OCH_2), 109.11 (CH_{ar}), 109.97 (CH_{ar}), 111.48 (CH_{ar}), 113.72 (CH_{ar}), 116.99 (CH_{ar}), 120.48 (CH_{ar}), 123.81 (CH_{ar}), 127.76 (CH_{ar}), 127.88 (CH_{ar}), 128.47 (CH_{ar}), 135.49 (C_{ar}), 137.25, 146.96, (C_{ar}), 148.82 (C_{ar}), 149.21 (C_{ar}), 150.85 ($C_{Pyrazoline}$), 154.29 (C_{ar}), 167.29 (C=O) ppm; MS (ESI$^+$, m/z): 483.2 (100.0%) [M + Na]$^+$; Anal. Calcd for $C_{27}H_{28}N_2O_5$: C, 70.42; H, 6.13; N, 6.08; Found: C, 70.58; H, 6.25; N, 6.19.

2.1.2.2. 1-(5-(4-(4-Fluorobenzyloxy)-3-methoxy phenyl)-4,5-dihydro-3-(3,4-dimethoxyphenyl) pyrazol-1-yl)ethanone (6b)

Yellowish brown solid; Yield (65%); mp 82-83 °C; (KBr) υ_{max}: 3071, 2936, 1659 cm^{-1}; ^{1}H NMR (400 MHz, DMSO-d_6) δ: 2.30 (s, 3H, CO-CH_3), 3.14 (dd, *J* = 4.0 Hz, *J* = 12.0 Hz, 1H, $H_{pyrazoline}$), 3.75 (s, 3H, OCH_3), 3.80 (s, 3H, OCH_3), 3.81 (s, 3H, OCH_3), 3.84-3.86 (m, 1H, $H_{pyrazoline}$), 5.01 (s, 2H, OCH_2), 5.47 (dd, *J* = 4.0 Hz, *J* = 8.0 Hz, 1H, $H_{pyrazoline}$), 6.63 (d, *J* = 8.0 Hz, 1H, H_{ar}), 6.84 (s, 1H, H_{ar}), 6.95 (d, *J* = 8.0 Hz, 1H, H_{ar}), 7.00 (d, *J* = 8.0 Hz, 1H, H_{ar}), 7.20 (t, *J* = 8.4 Hz, 2H, H_{ar}), 7.28 (d, *J* = 8.0 Hz, 1H, H_{ar}), 7.36 (s, 1H, H_{ar}), 7.45-7.48 (m, 2H, H_{ar}) ppm; ^{13}C NMR (100 MHz, DMSO-d_6) δ: 21.73 (CO-$\underline{C}H_3$), 42.23 ($CH_{Pyrazoline}$), 55.50 (OCH_3), 55.57 (OCH_3), 59.04 ($CH_{Pyrazoline}$), 69.28 (OCH_2), 109.11 (CH_{ar}), 109.95 (CH_{ar}), 111.44 (CH_{ar}), 113.84 (CH_{ar}), 115.09 (d, $^2J_{CF}$ = 21.0 Hz, $\underline{C}H_{ar}$-$C_{ar}F$), 116.96 (CH_{ar}), 120.38 (CH_{ar}), 129.82 (d, $^3J_{CF}$ = 8.0 Hz, $\underline{C}H_{ar}$-CH_{ar}-$C_{ar}F$), 133.42 (C_{ar}), 133.45 (C_{ar}), 135.59 (C_{ar}), 146.78 (C_{ar}), 148.77 (C_{ar}), 149.20 (C_{ar}), 150.79 ($C_{Pyrazoline}$), 154.15 (C_{ar}), 160.53 (d, $^1J_{CF}$ = 242.0 Hz, C_{ar}-F), 167.17 (C=O) ppm; ^{13}C DEPT-135 (100 MHz, DMSO-d_6) δ: 21.51 (CO-$\underline{C}H_3$), 42.01 ($CH_{Pyrazoline}$), 55.28 (OCH_3), 55.36 (OCH_3), 58.82 ($CH_{Pyrazoline}$), 69.06 (OCH_2), 108.88 (CH_{ar}), 109.73 (CH_{ar}), 111.22 (CH_{ar}), 113.61 (CH_{ar}), 114.87 (d, $^2J_{CF}$ = 22.0 Hz, $\underline{C}H_{ar}$-$C_{ar}F$), 116.73 (CH_{ar}), 120.18 (CH_{ar}), 129.61 (d, $^3J_{CF}$ = 9.0 Hz, $\underline{C}H_{ar}$-CH_{ar}-$C_{ar}F$) ppm; Anal. Calcd for $C_{27}H_{27}FN_2O_5$: C, 67.77; H, 5.69; N, 5.85; Found: C, 67.86; H, 5.78; N, 5.96.

2.1.2.3. 1-(5-(4-(Benzyloxy)-3-methoxyphenyl)-4,5-dihydro-3-(3,4,5-trimethoxyphenyl)pyrazol-1-yl)ethanone (6c)

Brown solid; Yield (64%); mp 68-69 °C; IR (KBr) υ_{max}: 3063, 2936, 1659 cm^{-1}; ^{1}H NMR (400 MHz, DMSO-d_6) δ: 2.32 (s, 3H, CO-CH_3), 3.22 (dd, *J* = 4.0 Hz, *J* = 12.0 Hz, 1H, $H_{pyrazoline}$), 3.70 (s, 3H, OCH_3), 3.76 (s, 3H, OCH_3), 3.77-3.79 (m, 1H, $H_{pyrazoline}$), 3.83 (s, 6H, 2 OCH_3), 3.87 (s, 3H, OCH_3,), 5.04 (s, 2H OCH_2), 5.49 (dd, *J* = 4.0 Hz, *J* = 8.0 Hz, 1H, $H_{pyrazoline}$), 6.63 (d, *J* = 8.4 Hz, 1H, H_{ar}), 6.84 (s, 1H, H_{ar}), 6.95 (d, *J* = 8.4 Hz, 1H, H_{ar}), 7.05 (s, 1H, H_{ar}), 7.16 (s, 1H, H_{ar}), 7.36-7.41 (m, 5H, H_{ar}) ppm; ^{13}C NMR (100 MHz, DMSO-d_6) δ: 21.73 (CO-$\underline{C}H_3$), 42.27 ($CH_{Pyrazoline}$), 55.61 (OCH_3), 55.99 (OCH_3), 59.24 (OCH_3), 60.14 ($CH_{Pyrazoline}$), 69.98 (OCH_2), 104.11 (CH_{ar}), 109.95 (CH_{ar}), 113.77 (CH_{ar}), 116.94 (CH_{ar}), 126.64 (CH_{ar}), 127.66 (CH_{ar}), 127.79 (C_{ar}), 127.86 (CH_{ar}), 128.40 (CH_{ar}), 128.41 (CH_{ar}), 135.43 (C_{ar}), 137.22 (C_{ar}), 139.43 (C_{ar}), 146.94 (C_{ar}), 149.22 ($C_{Pyrazoline}$), 153.02 (C_{ar}), 154.19 (C_{ar}), 167.35 (C=O) ppm; Anal. Calcd for $C_{28}H_{30}N_2O_6$: C, 68.56; H, 6.16; N, 5.71; Found: C, 68.67; H, 6.27; N, 5.80.

2.1.2.4. 1-(5-(4-(4-Methylbenzyloxy)-3-methoxy phenyl)-4,5-dihydro-3-(3,4,5-trimethoxy phenyl)pyrazol-1-yl)ethanone (6d)

Brown solid; Yield (67%); mp 89 °C; IR (KBr) υ_{max}: 3001, 2932, 1659 cm^{-1}; ^{1}H NMR (400 MHz, DMSO-d_6) δ: 2.29 (s, 3H, CH_3), 2.30 (s, 3H, CO-CH_3), 3.13 (dd, *J* = 4.0 Hz, *J* = 12.0 Hz, 1H, $H_{pyrazoline}$), 3.74 (s, 3H, OCH_3), 3.80 (s, 3H, OCH_3), 3.81 (s, 6H, 2 OCH_3), 3.85 (d, *J* = 4.0 Hz, 1H, $H_{pyrazoline}$), 4.98 (s, 2H, OCH_2), 5.46 (dd, *J* = 4.0 Hz, *J* = 8.0 Hz , 1H, $H_{pyrazoline}$), 6.82 (s, 1H, H_{ar}), 6.93 (d, *J* = 8.4 Hz, 1H, H_{ar}), 7.01 (d, *J* = 8.4 Hz, 1H, H_{ar}), 7.16-7.18 (m, 2H, H_{ar}), 7.29-7.35 (m, 4H, H_{ar}) ppm; ^{13}C NMR (100 MHz, DMSO-d_6) δ: 20.78 (CH_3), 21.76 (CO-$\underline{C}H_3$), 42.26 ($CH_{Pyrazoline}$), 55.54 (OCH_3), 55.61 (OCH_3), 59.06 ($CH_{Pyrazoline}$), 69.86 (OCH_2), 109.14 (CH_{ar}), 109.98 (CH_{ar}), 111.48 (CH_{ar}), 113.74 (CH_{ar}), 116.97 (CH_{ar}), 120.42 (CH_{ar}), 123.79 (CH_{ar}), 127.80 (CH_{ar}), 127.98 (C_{ar}), 128.00 (C_{ar}), 128.96 (CH_{ar}), 134.17 (C_{ar}), 135.37 (C_{ar}), 137.06 (C_{ar}), 146.95 (C_{ar}), 148.80 (C_{ar}), 149.19 (C_{ar}), 150.82 ($C_{Pyrazoline}$), 154.21 (C_{ar}), 167.22 (C=O) ppm; Anal. Calcd for $C_{29}H_{32}N_2O_6$: C, 69.03; H, 6.39; N, 5.55; Found: C, 69.18; H, 6.47; N, 5.67.

2.2. Biology:

The Medical Research Ethics Committee at National Research Centre - Egypt has approved this study with Ethical Approval Number: **19280**.

2.2.1. Anticancer activity:

2.2.1.1. Cell culture:

Two human hepatoma cell lines (HuH-7, and HepG-2) and a normal hepatocyte cell line (BNL) (Nawah Scientific Inc., Cairo, Egypt) were grown in Dulbecco's Modified Eagle Medium (DMEM) media supplemented with streptomycin (100 mg/mL), penicillin (100 units/mL), and heat-inactivated fetal bovine serum (10% FBS) in dampened atmosphere with 5% CO_2 at 37 °C [39].

2.2.1.2. Cytotoxicity assay:

Cell suspension (100 µL of 4 x10^3 cells /well) was seeded in 96-well plates, incubated overnight, and treated with serial dilutions of test compounds **(6a-d)** for 72 hours. Then, cells were fixed by adding trichloroacetic acid (150 µL of 10% TCA) for one hour at 4°C. To dissolve the protein-bound sulforhodamine B (SRB) stain, we added 150 µL of tris base (10 mM) and measured absorbance at 540 nm with a microplate reader (FLUOstar Omega, Ortenberg, Germany). IC_{50} values are measured as mean ± SD. The selectivity index (SI), the cytotoxic selectivity for the proposed treatments, was reported as SI = IC_{50} of normal cells / IC_{50} of cancer cells [40].

2.2.2. NCI-60 anticancer screening:

All the newly synthesized *N*-acetylpyrazolines **6a-d** were selected and screened by the Developmental Therapeutic Program (DTP) at the National Cancer Institute (NCI) in Bethesda, Maryland, US [41-48]. The anticancer screening results were reported as growth inhibition percentage (GI) % at 10 µM.

2.2.3. Tubulin polymerization assay:

Tubulin polymerization assay kit (Cat. BK006P, Cytoskeleton, Inc., US) was used, and the experimental protocol was done according to manufacturer [49]. Paclitaxel, a microtubules stabilizing agent, and combrestatin A-4 (CA-4), a microtubules destabilizing agent, were purchased from Sigma Aldrich, and used as positive controls. The direct effect of compounds **6a-d** on tubulin polymerization was determined in an *in vitro* fluorescent-based assay (Cytoskeleton, Denver, CO). Briefly, in 96-well plates tubulin reaction mix (2 mg/ml porcine brain tubulin in 80 nM Pipes, pH 6.9, 2 nM $MgCl_2$, 0.5 mM EGTA, 1 mM GTP and 15% glycerol) were used to dilute each 10x compounds. Fluorescence changes were monitored kinetically in the Cytation 3 Multi-Mode Reader (Biotek, Canada) at 37 °C for 1 h, one read per minute, using excitation at 360 nm and emission at 420 nm.

2.3. Molecular docking study:

Molecular docking simulations were performed using Molecular Operating Environment software (MOE, 2022.02), using high-resolution cryo-EM reconstruction of Taxol-stabilized microtubule (PDB ID: 5SYF) [50, 51]. The detailed docking protocol was reported in supporting information.

2.4. Prediction of physicochemical and ADME properties as well as drug-likeness and medicinal chemistry friendliness:

SwissADME online web tool was employed to predict the physicochemical and ADME properties as well as drug-likeness and medicinal chemistry friendliness of the target compounds **6a-d**. The compounds' SMILES were generated utilizing (MOE, 2022.02) software then they were submitted to *SwissADME* [52-54].

3. Results and Discussion

3.1. Chemistry:

The target compounds **6a-d** were synthesized *via* the reaction of the previously synthesized *p*-benzyloxy-3-methoxybenzaldehydes **3a-c** according to reported method [55-57] and 3',4'-dimethoxyacetophenone **4a** or 3',4',5'-trimethoxyacetophenone **4b** through Claisen-Shmidt condensation reaction forming the novel chalcones **5a-d** using 50% aqueous potassium hydroxide. The synthesized chalcones **5a-d** was cyclized using hydrazine hydrate in the presence of glacial acetic acid forming the novel *N*-acetylpyrazolines **6a-d** (Scheme 1). Chalcones **5a-d** were found in (*E*) configuration based on the coupling constant (J = 12-16 Hz) for the α,β-unsaturated ketone protons. The ^{13}C DEPT-135 (Distortionless Enhancement by Polarisation Transfer) spectrum of the *N*-acetylpyrazoline derivative **6b** was performed to confirm the presence of the methylene group of the 4,5-dihydropyrazole ring that resonated at 42.01 ppm, whereas, the OCH_2 group at 69.06 ppm in the negative/inverted mode, while, the methyl and methine carbons resonated in the positive/upright

mode (Figure 3). For ^{1}H and ^{13}C NMR, and mass spectral data of the synthesized chalcones **5a-d**, and *N*-acetylpyrazolines **6a-d**, see supporting information (Figures S.1-S.19).

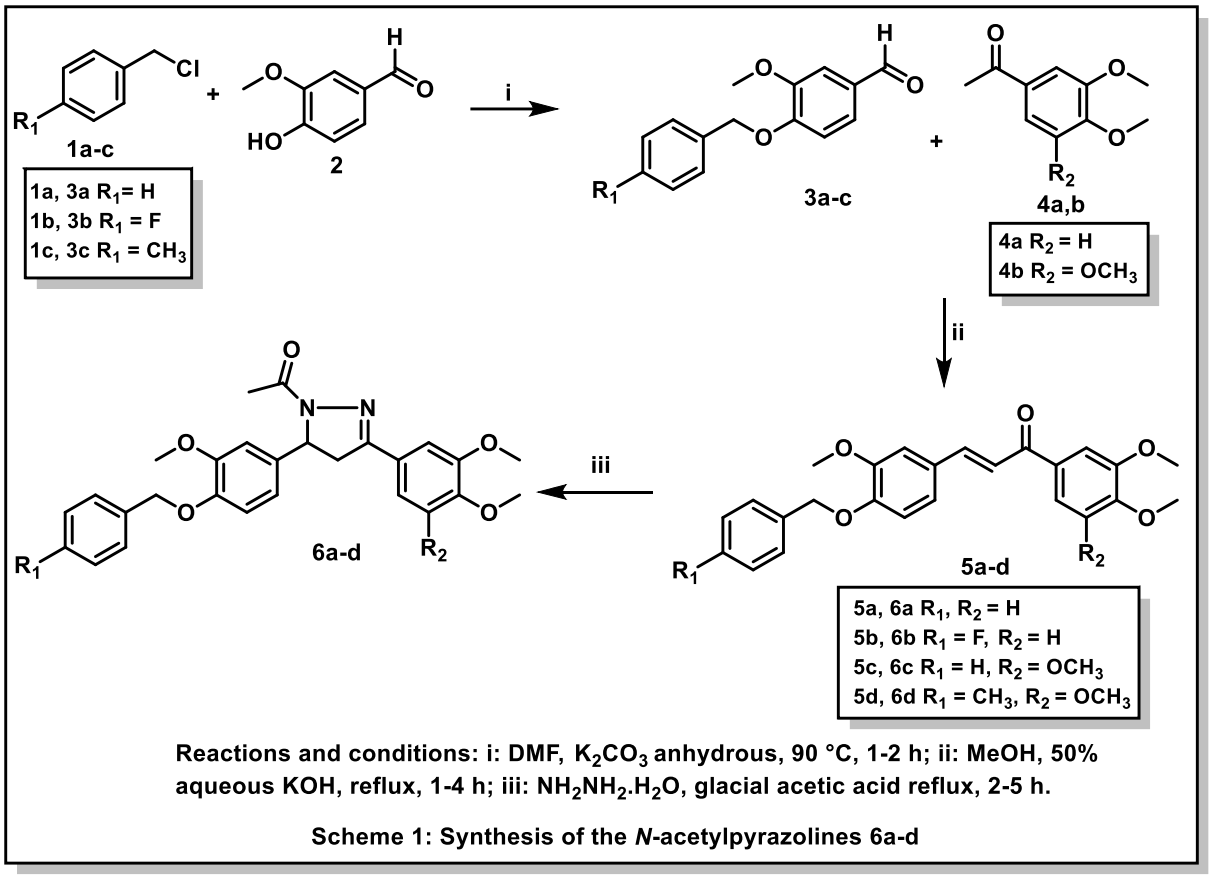

Reactions and conditions: i: DMF, K_2CO_3 anhydrous, 90 °C, 1-2 h; ii: MeOH, 50% aqueous KOH, reflux, 1-4 h; iii: $NH_2NH_2.H_2O$, glacial acetic acid reflux, 2-5 h.

Scheme 1: Synthesis of the *N*-acetylpyrazolines 6a-d

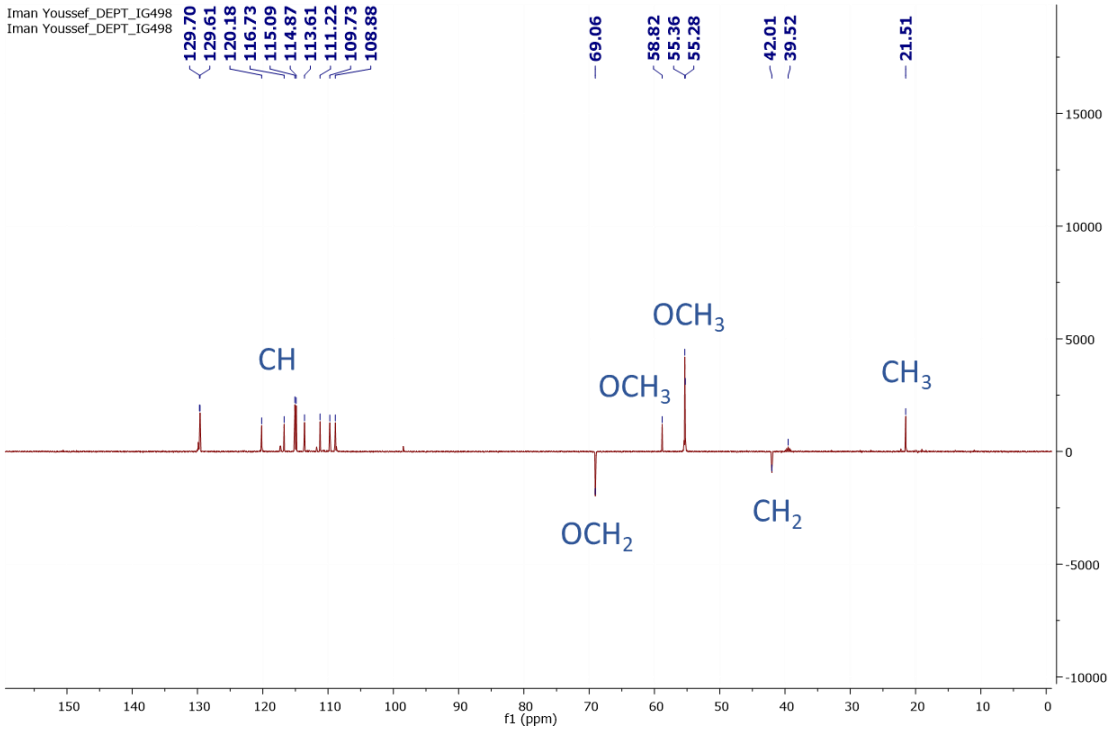

Figure 3: ^{13}C DEPT-135 spectrum of the *N*-acetylpyrazoline **6b**

3.2. Biology

3.2.1. Anticancer activity against HuH-7, HepG-2, and BNL cell lines:

The cytotoxic activity of compounds **6a-d** was first evaluated against liver cancer cells (HuH-7, and HepG-2) and normal cells (BNL) at two concentrations (10 and 100 µM). Growth inhibition percentage (GI%) was calculated and compared to paclitaxel, colchicine, and CA-4 as standards (**Table 1**).

Compounds **6a-d** inhibited growth in HuH-7 liver cancer cells with GI% values of 12.1-39.4% and 65.2-82.9% at 10 and 100 µM, respectively. However, they had lower GI% values against HepG-2 cells at both concentrations (6.0-22.3% and 36.7-51.3%), indicating that compounds **6a-d** had more potent anticancer activity against the HuH-7 cell line than the HepG-2 cell line. Furthermore, the four synthesized compounds **6a-d** were further tested for IC_{50} determination (**Table 2**). The results depicted that the 3',4',5'-trimethoxyphenyl *N*-acetylpyrazolines (**6c** and **6d**) showed more potent anticancer activity than the 3',4'-dimethoxyphenyl pyrazolines (**6a** and **6b**) with IC_{50} values of 11.00 and 0.30 µM vs 50.20 and 14.50 µM, respectively against the HuH-7 cell line. Regarding the HepG-2 cell line, only compounds **6b** and **6d** showed weak to moderate anticancer activities with IC_{50} values of 90.00 and 77.30 µM, respectively. While compounds **6a** and **6c** didn't show noticeable cytotoxicity till the concentration of 100 µM. Fortunately, all the tested compounds **6a-d** showed IC_{50} values of more than 100 µM against the normal mouse BNL liver cell line and their selectivity index values were calculated and presented in Table 2, confirming the active targeting power of the pyrazoline compounds against the cancerous cells while providing the safety of normal cells [58, 59]. The tested compounds displayed the highest selectivity and potency towards HuH-7 cells rather than HepG-2 cells. Among them, compound **6d** was the safest compound (SI = > 333 and 1.29 for HuH-7 and HepG-2, respectively). The IC_{50} graphs for compounds **6b-d** are inserted in supporting information (Figures S.20-S.22).

Table 1
Growth inhibition (GI) % of compounds **6a-d** against liver cancer and normal cell lines at 10 and 100 µM.

Compound ID	HuH-7		HepG-2		BNL	
	GI%					
	10 µM	100 µM	10 µM	100 µM	10 µM	100 µM
6a	12.1	65.4	6.0	6.98	1.45	4.52
6b	39.4	82.9	22.3	54.7	2.5	6.5
6c	33.8	89.2	5.31	8.65	0.94	2.87
6d	88.8	99.4	17.3	64.0	5.21	7.59
Paclitaxel	81.0	99.91	88.85	97.2	97.4	100.9
Colchicine	89.4	99.63	56.33	93.8	90.3	100.1
CA-4	80.0	99.0	86.22	98.4	88.5	99.99

Table 2
IC_{50} values of compounds **6a-d** against HepG-2, HuH-7, and BNL cell lines and the selectivity index (SI).

Compound ID	HuH-7	HepG-2	BNL	HuH-7	HepG-2
	IC_{50} (µM)			SI	
6a	50.20	>100	>100	> 1.99	> 1
6b	14.50	90.00	>100	> 6.89	> 1.1
6c	11.00	>100	>100	> 9.09	> 1
6d	0.30	77.30	>100	> 333	1.29
Paclitaxel	0.02	1.10	0.001	0.05	0.001
Colchicine	0.056	6.61	0.014	0.25	0.002
CA-4	0.026	1.47	0.499	19.19	0.339

3.2.2. NCI-60 anticancer screening:

All the newly synthesized *N*-acetylpyrazolines **6a-d** were screened for their possible anticancer activity by the National Cancer Institute (NCI - US) against a cancer cell lines panel *via* a sulforhodamine B (SRB) assay.

Table 3 presents the growth inhibition (GI) percentage of the target compounds **6a-d** at 10 µM. The one-dose mean graphs were presented in supporting information (Figures S.23-S.26). The *N*-acetylpyrazolines **6a-d** showed mean GI% values of 8.87, 46.54, 64.54, and 54.63%, respectively. The 3',4'-dimethoxyphenyl analogue **6a** showed the lowest anticancer activity among the synthesized *N*-acetylpyrazolines with GI% of 8.87%, while, it revealed a moderate anticancer activity against lung (EKVX, and NCI-H522), colon (HCT-15), melanoma (UACC-62), renal (UO-31), and breast (MCF-7, and T-47D) cancer cell lines with GI% values 31.83, 40.68, 30.09, 36.80, 38.14, 32.39, and 39.94%, respectively. The *N*-acetylpyrazolines **6b-d** showed moderate to high and broad anticancer activities against leukemia (K-562, and MOLT-4), lung (A-549, HOP-92, and NCI-H522), colon (COLO 205, HCT-116, HCT-15, and HT 29), CNS (SF-295), melanoma (SK-MEL-5), ovarian (OVCAR-4), renal (UO-31), prostate (PC-3), and breast (MCF-7, HS 578T, BT-549, T-47D, and MDA-MB-468) cancer cell lines with GI% ranges (69.04-91.21%), (49.24-104.80%), (41.53-89.09%), (62.17-75.38%), (70.31-109.52%), (57.92-77.71%), (70.26-91.37%), (72.34-90.16), and (39.94-97.30%), respectively. Moreover, the 3',4',5'-trimethoxyphenyl *N*-acetylpyrazoline **6c**, and **6d** revealed not only potent anticancer activities but also nearly complete lethal effects against lung cancer cell line (HOP-92) for **6c** and melanoma cell line (SK-MEL-5) for **6d** with GI% values of 104.80, and 109.52%, respectively.

3.2.3. Tubulin polymerization assay:

All the synthesized *N*-acetylpyazolines **6a-d** were tested at 50 µM on tubulin polymerization assay, and the emmission used at 420 nm for 1 h. Paclitaxel, a tubulin stabilizing agent (10 µM), and CA-4 (10 µM), a tubulin destabilizing agent, were used as positive controls for the tubulin polymerization assay. The *N*-acetylpyrazolines **6a-d** showed tubulin-stabilizing effects as paclitaxel at 50 µM (Figures 4, and 5). The 3',4',5'-trimethoxyphenyl *N*-acetylpyrazoline **6d** was further tested for EC_{50} (µM) values determination in comarison to paclitaxel, and it was found its EC_{50} value > 100 µM (Figure 6).

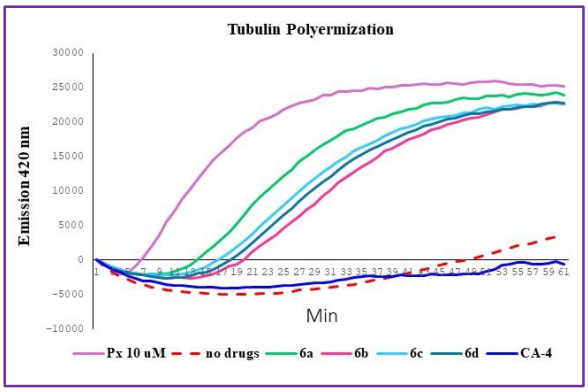

Figure 4: Microtubule-stabilizing effects of compounds **6a-d** at 50 µM vs paclitaxel, and CA-4 at 10 µM.

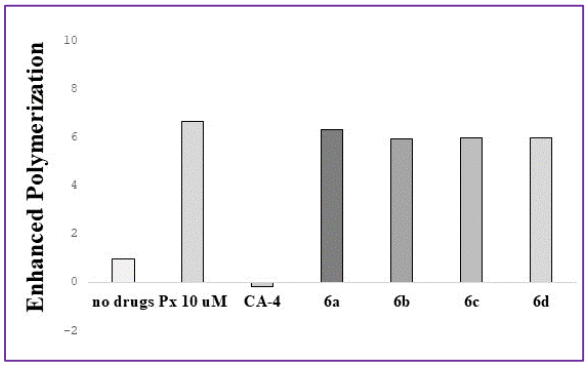

Figure 5: Enhanced tubulin polymermization for compounds **6a-d** at 50 µM.

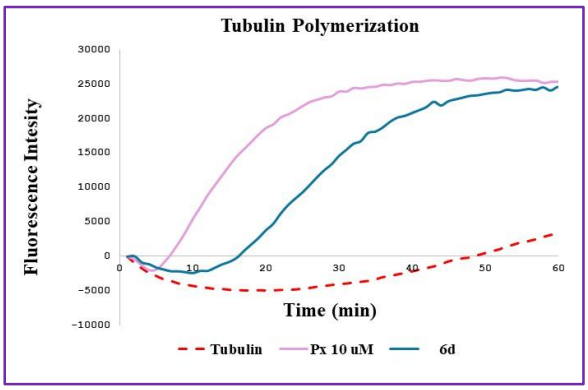

Figure 6: EC_{50} graph of compound **6d** on tubulin polymerization

Table 3
Growth inhibition (GI) % of compounds **6a-d** against a panel of cancer cell lines at 10 µM.

Subpanel of Cancer Cell Lines	Compound ID								
	6a	**6b**	**6c**	**6d**		**6a**	**6b**	**6c**	**6d**
	GI%								
Leukemia					**Melanoma Cont.**				
CCRF-CEM	nd[a]	40.11	59.84	49.93	MDA-MB-435	-	37.52	55.43	56.95
HL-60(TB)	nd	62.68	78.49	65.37	SK-MEL-2	5.38	30.49	78.74	55.88
K-562	nd	72.04	81.36	69.04	SK-MEL-28	-	26.77	57.90	43.24
MOLT-4	nd	69.37	91.21	79.51	SK-MEL-5	-	70.31	90.23	109.52
PRMI-8226	5.96	63.43	75.83	63.02	UACC-257	-	31.38	51.22	59.85
SR	nd	60.34	67.93	47.61	UACC-62	36.80	47.96	75.95	65.96
Non-Small Cell Lung Cancer					**Ovarian Cancer**				
A549/ATTC	25.08	49.24	68.18	70.97	IGROV1	24.44	54.19	57.07	51.03
EKVX	31.83	40.55	67.37	53.72	OVCAR-3	-	29.69	59.03	58.58
HOP-62	-[b]	25.78	29.77	23.77	OVCAR-4	--	57.92	77.71	70.62
HOP-92	11.47	82.67	104.80	62.88	OVCAR-5	--	42.22	40.15	20.16
NCI-H226	-	50.18	72.02	50.06	OVCAR-8	19.41	38.07	53.32	56.51
NCI-H23	-	43.35	52.81	41.95	NCI/ADR-RES	-	31.36	61.56	43.90
NCI-H322M	8.33	33.88	40.21	18.14	SK-OV-3	-	48.05	28.72	15.06
NCI-H460	-	50.97	75.73	58.72	**Renal Cancer**				
NCI-H522	40.68	57.91	73.16	71.47	786-0	5.47	42.24	66.03	42.11
Colon Cancer					A498	-	40.61	44.91	35.09
COLO 205	--[c]	41.53	89.09	58.70	ACHN	10.68	40.80	71.80	57.12
HCC-2998	-	13.98	28.76	16.63	CAKI-1	19.33	46.78	70.69	52.83
HCT-116	22.18	68.50	75.69	64.69	RXF 393	-	26.33	68.62	47.05
HCT-15	30.09	57.51	65.42	72.09	SN 12C	22.36	46.10	58.93	56.84
HT29	23.64	71.90	61.69	59.94	TK-10	8.67	49.49	67.91	55.94
KM12	12.70	42.85	66.11	61.01	UO-31	38.14	70.26	91.37	77.61
SW-620	-	41.46	44.91	38.80	**Prostate Cancer**				
CNS Cancer					PC-3	18.61	72.34	90.16	76.39
SF-268	17.22	28.04	52.21	52.89	DU-145	-	29.37	59.56	48.71
SF-295	22.94	62.35	75.38	62.17	**Breast Cancer**				
SF-539	7.46	38.12	48.30	36.23	MCF7	32.39	65.33	82.89	79.86
SNB-19	19.71	39.14	47.82	48.59	MDA-MB-231/ATTC	15.32	39.00	35.98	30.41
SNB-75	-	20.51	50.68	38.73	HS 578T	--	41.22	58.98	43.74
U251	9.74	40.10	55.69	53.22	BT-549	nd	55.12	82.62	66.20
Melanoma					T-47D	39.94	39.94	75.17	97.30
MALME-3M	--	18.16	56.88	51.92	MDA-MB-468	6.14	52.90	65.76	68.93
M14	--	40.13	63.09	45.78					
Mean GI %	**8.87**	**46.54**	**64.77**	**54.63**					

[a]: Not determined.
[b]: No GI% detected at 10 µM.
[c]: GI% lower than 5%.

3.3. Molecular docking study:

Molecular dockings simulations were performed to investigate the binding pattern of the newly synthesized compounds **6a-d** at the Taxol-binding-site of the microtubule and to explain their promising microtubule-stabilizing activity. In the current study, high-resolution cryo-EM reconstruction of Taxol-stabilized microtubule (PDB ID: 5SYF) was utilized to perform the molecular docking simulations [50, 51]. Primarily, self-docking validation was carried out to validate the used docking protocol by docking Taxol at its binding site on the microtubule. The self-docking validation step accurately regenerated the interaction pattern of Taxol in its binding site showing that the used docking setup is appropriate for the intended docking study. This is demonstrated by the small RMSD value between the co-crystalized inhibitor and its docking pose (1.550Å) and by the capability of the attained pose to duplicate the key interactions achieved by the co-crystalized pose with the residues His229, Thr276, and Arg369 (Figure 7 and 8). In its binding site, Taxol interacts through Van der Waals interactions by its 3′-benzoyl moiety with β-tubulin His229. Furthermore, through hydrogen bonding, it interacts by its 3′-oxygen, 2′-OH, and oxetane ring oxygen with His229 nitrogen, Arg369 backbone carbonyl, and Thr276 (in strand S7) backbone NH, respectively (Figure 7 and 8).

Compared to the natural ligand, the *N*-acetylpyrazoline derivatives **6a-d** showed a predicted docking energy score (S) range of −9.97 to −10.49 kcal/mol (Table 4). The tested compounds 6a-d showed a comparable predicted binding affinity which agrees with their experimental activity. Compounds **6a-d** showed a common binding pattern in Taxol-binding-site interacting with the key amino acid Thr276 (in strand S7) (Figures 9-12). The binding pattern involves the fitting of the *N*-acetylpyrazoline ring in the Taxol's oxetane ring region achieving H-bond interaction with the key amino acid Thr276. On one side directing the hydrophobic (un)substituted benzyloxy phenyl moiety, in the region of Taxol's 3′-phenyl moiety, deeply towards the hydrophobic subpacket in the tubulin beta subunit lined by the hydrophobic side chains of the amino acids Val23, Ala233, Phe272, Pro274, Pro360, and Leu371. On the other side directing the (di)(tri)methoxyphenyl moiety towards Arg278 interacting *via* hydrophobic interaction with Leu217 and Leu219 of the side chains (Figures 9-12).

Table 4
Docking scores (*S*) in kcal/mol for the *N*-acetylpyrazolines **6a-d** and Taxol in microtubule binding sites.

Compound ID	Docking score (*S*) (kcal/mol)
Paclitaxel	−12.75
6a	−10.49
6b	−10.11
6c	−9.97
6d	−10.12

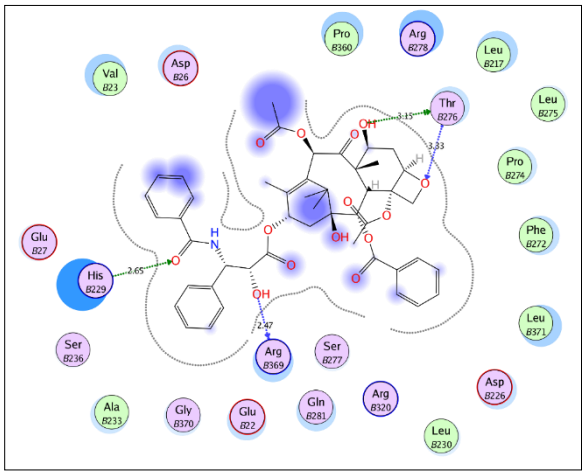

Figure 7: 2D interaction diagram showing Taxol docking pose interactions with the key amino acids in Taxol-binding-site on the microtubule (Distance in Å).

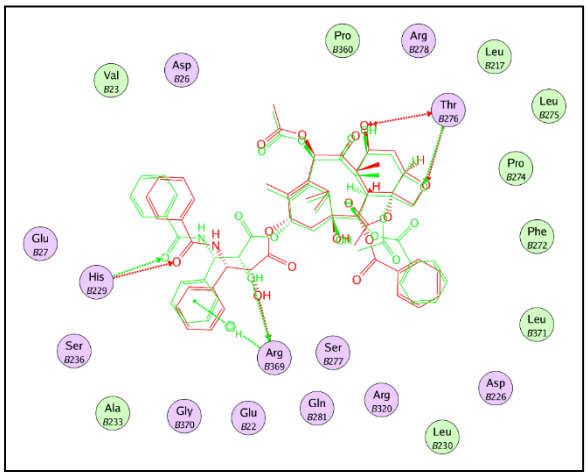

Figure 8: 2D Superimposition diagram of the co-crystallized (red) and the docking pose (green) of Taxol in Taxol-binding-site on the microtubule with RMSD of 1.550Å.

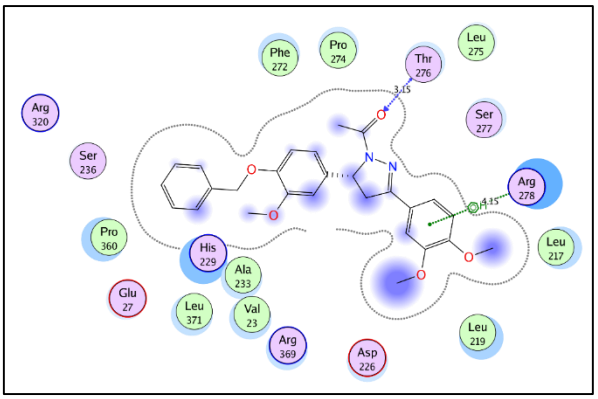

(A)

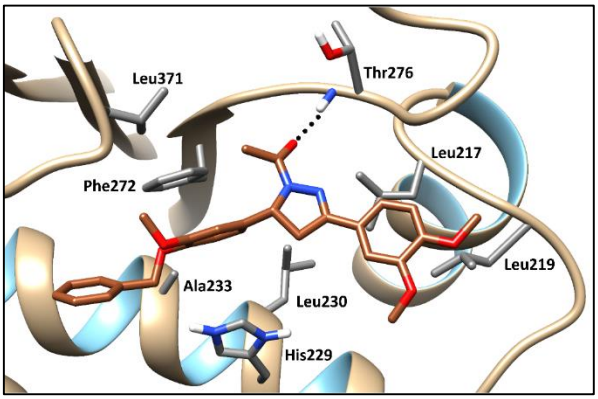

(B)

Figure 9: 2D interaction diagram (A) and 3D representation (B) showing interactions of compound **6a** docking pose at the Taxol site on the microtubule. (Distances in Å)

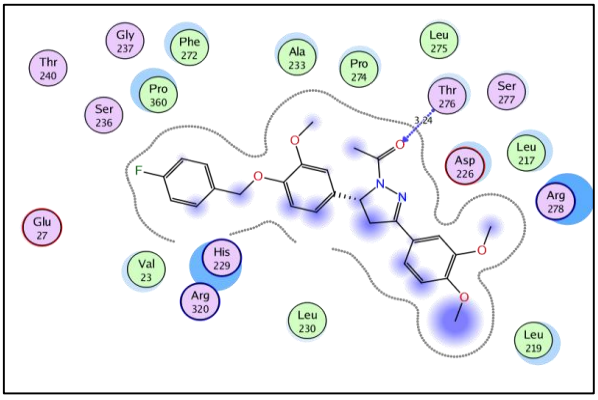

(A)

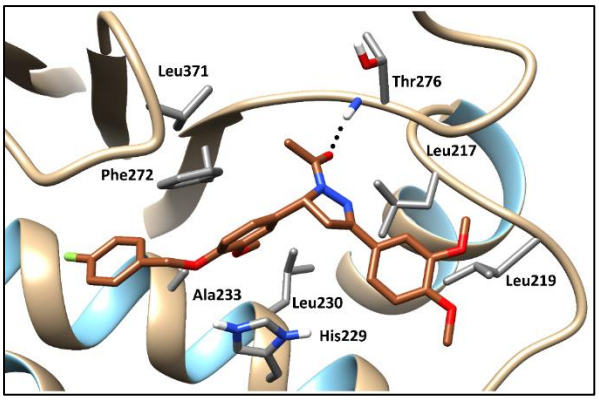

(B)

Figure 10: 2D interaction diagram (A) and 3D representation (B) showing interactions of compound **6b** docking pose at the Taxol site on the microtubule. (Distances in Å)

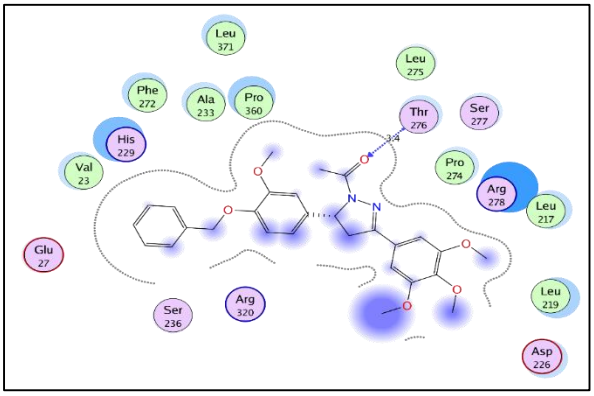

(A)

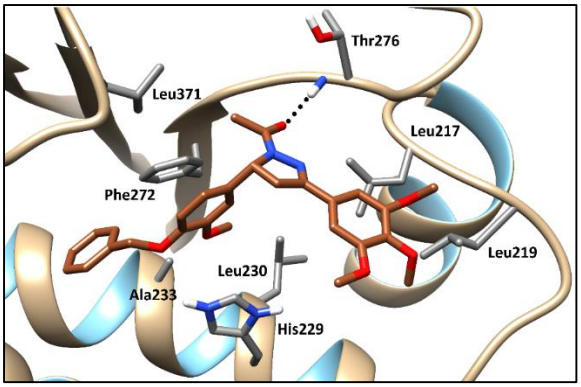

(B)

Figure 11: 2D interaction diagram (A) and 3D representation (B) showing interactions of compound **6c** docking pose at the Taxol site on the microtubule. (Distances in Å)

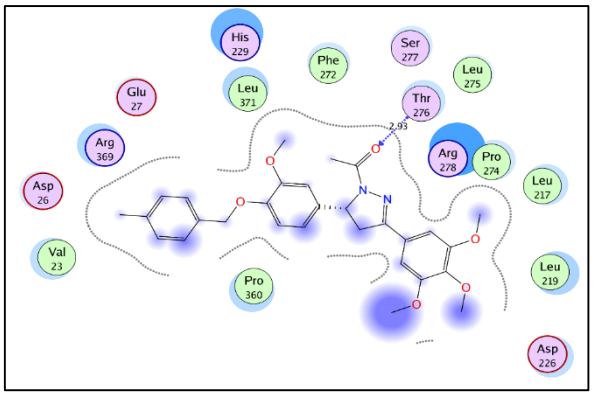

(A)

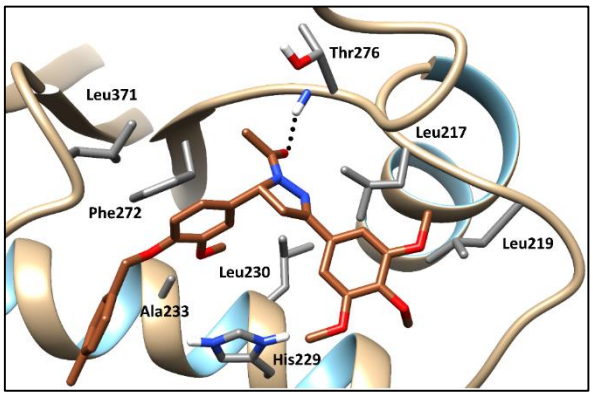

(B)

Figure 12: 2D interaction diagram (A) and 3D representation (B) showing interactions of compound **6d** docking pose at the Taxol site on the microtubule. (Distances in Å)

3.4. Prediction of physicochemical and ADME properties as well as drug-likeness and medicinal chemistry friendliness of compounds 6a-d:

The promising activity of the *N*-acetylpyrazolines **6a-d** encouraged us to further predict their physicochemical and ADME properties as well as their drug-likeness and medicinal chemistry friendliness. As a result, the *SwissADME* web tool provided by the Swiss Institute of Bioinformatics (SIB) was utilized [52-54].

As can be seen in **table 5**, compounds **6a-d** exhibited promising physicochemical properties displaying molecular weight range of 460.52 – 504.57 Da, rotatable bond number of 9 or 10, topological polar surface area (TPSA) of 69.59 or 78.52 $Å^2$ which is less than the cutoff for oral bioavailability (140 $Å^2$) [60] and a predicted consensus logP range of 4.00-4.35. Furthermore, the target compounds predicted to be moderately water soluble according to log S model from Ali J. *et al.*, [61]. For further details see supporting materials. Predicted ADME properties showed that the target compounds **6a-d** are highly GIT absorbable. Furthermore, compounds **6c-d** showed no predicted BBB permeation and so with no predicted CNS side effects, however, **6a-b** analogues predicted to be able to pass BBB. All compounds were predicted to be P-gp substrates (For further details see supporting materials).

As for their drug-likeness, the target compounds adhered to Lipinski's rule of five, with at most one violation (**Table 5**). Additionally, they exhibited a favourable Abbott bioavailability score of 0.55 [62]. All the target compounds showed a promising medicinal chemistry friendliness with no pan assay interference compounds (PAINS) alerts [63] in their structures and with reasonable synthetic accessibility ranging 4.22 – 4.53 (1 is easy to synthesize and 10 is difficult) (For further details see supporting materials).

Table 5
SwissADME predicted physicochemical and drug-likeness properties.

Compound ID	MW	#Rot. bond	#H-bond acc.	#H-bond don.	TPSA	Cons. LogP	#Lipinski's violations
6a	460.52	9	6	0	69.59	4.02	0
6b	478.51	9	7	0	69.59	4.35	0
6c	490.55	10	7	0	78.82	4.00	0
6d	504.57	10	7	0	78.82	4.34	1

4. Conclusion

New *N*-acetylpyrazoline derivatives **6a-d** were synthesized *via* the reaction of corresponding chalcones **5a-d** and hydrazine hydrate in acidic medium. The synthesized pyrazolines were evaluated *in vitro* for their anticancer activity against liver (HuH-7, and HepG-2) cancer and (BNL) normal cell lines. The *N*-acetylpyrazolines **6b-d** revealed potent anticancer activity against HuH-7 cell line IC_{50} = 14.50, 11.00, and 0.30 µM, respectively. Compounds **6a-d** were further screened for their anticancer potential against different cancer cell lines at 10 µM, and the 3',4',5'-trimethoxyphenyl *N*-acetylpyrazoline **6d** revealed potent anticancer activities mean GI% (64.54%). Moreover, the *N*-acetylpyrazolines **6a-d** were tested for their effects on tubulin polymerization at 50 µM compared to paclitaxel, and CA-4 as standards, whereas, they showed tubulin stabilizing effects similar to paclitaxel. A molecular docking study was performed to investigate the binding pattern of the *N*-acetylpyrazolines **6a-d** at the Taxol-binding site of microtubules. A predicted ADME properties study showed that compounds **6a-d** are highly GIT absorbable without predicted BBB permeation and so with no predicted CNS side effects.

5. Conflicts of interest

"There are no conflicts to declare".

6. Formatting of funding sources

The authors are thankful for the National Research Centre (NRC) - Egypt under the research grant (Project ID: **12010107**) for the financial support of this work.

7. Acknowledgments

The authors are thankful the National Cancer Institute (NCI) - USA for the antitumor testing of the synthesized pyrazolines.

8. References

[1] M.M. Fakhry, A.A. Mattar, M. Alsulaimany, E.M. Al-Olayan, S.T. Al-Rashood, H.A. Abdel-Aziz, New Thiazolyl-Pyrazoline Derivatives as Potential Dual EGFR/HER2 Inhibitors: Design, Synthesis, Anticancer Activity Evaluation and In Silico Study, Molecules, 28 (2023) 7455.
[2] B.S. Chhikara, K. Parang, Global Cancer Statistics 2022: the trends projection analysis, Chem Biol Lett, 10 (2023) 451.
[3] A. Villanueva, Hepatocellular Carcinoma, N Engl J Med, 380 (2019) 1450-1462.
[4] J.M. Llovet, R.K. Kelley, A. Villanueva, A.G. Singal, E. Pikarsky, S. Roayaie, R. Lencioni, K. Koike, J. Zucman-Rossi, R.S. Finn, Hepatocellular carcinoma, Nat Rev Dis Primers, 7 (2021) 6.
[5] H. Wege, K. Schulze, J. von Felden, J. Calderaro, M. Reig, Rare variants of primary liver cancer: Fibrolamellar, combined, and sarcomatoid hepatocellular carcinomas, Eur J Med Genet, 64 (2021) 104313.
[6] K. Nepali, R. Ojha, S. Sharma, P.M. Bedi, K.L. Dhar, Tubulin inhibitors: a patent survey, Recent Pat Anticancer Drug Discov, 9 (2014) 176-220.
[7] S. Sharma, C. Kaur, A. Budhiraja, K. Nepali, M.K. Gupta, A.K. Saxena, P.M. Bedi, Chalcone based azacarboline analogues as novel antitubulin agents: design, synthesis, biological evaluation and molecular modelling studies, Eur J Med Chem, 85 (2014) 648-660.
[8] H. Singh, M. Kumar, K. Nepali, M.K. Gupta, A.K. Saxena, S. Sharma, P.M.S. Bedi, Triazole tethered C5-curcuminoid-coumarin based molecular hybrids as novel antitubulin agents: Design, synthesis, biological investigation and docking studies, Eur J Med Chem, 116 (2016) 102-115.
[9] E. Nogales, M. Whittaker, R.A. Milligan, K.H. Downing, High-Resolution Model of the Microtubule, Cell, 96 (1999) 79-88.
[10] A. Farce, C. Loge, S. Gallet, N. Lebegue, P. Carato, P. Chavatte, P. Berthelot, D. Lesieur, Docking Study of Ligands into the Colchicine Binding Site of Tubulin, J Enzyme Inhib Med Chem, 19 (2004) 541-547.
[11] Y.-T. Wang, T.-Q. Shi, H.-L. Zhu, C.-H. Liu, Synthesis, biological evaluation and molecular docking of benzimidazole grafted benzsulfamide-containing pyrazole ring derivatives as novel tubulin

polymerization inhibitors, Bioorg Med Chem, 27 (2019) 502-515.
[12] Y.M. Liu, H.L. Chen, H.Y. Lee, J.P. Liou, Tubulin inhibitors: a patent review, Expert Opin Ther Pat, 24 (2014) 69-88.
[13] F. Naaz, M.R. Haider, S. Shafi, M.S. Yar, Anti-tubulin agents of natural origin: Targeting taxol, vinca, and colchicine binding domains, Eur J Med Chem, 171 (2019) 310-331.
[14] Y.N. Cao, L.L. Zheng, D. Wang, X.X. Liang, F. Gao, X.L. Zhou, Recent advances in microtubule-stabilizing agents, Eur J Med Chem, 143 (2018) 806-828.
[15] M.M. Hammouda, A. Abo Elmaaty, M.S. Nafie, M. Abdel-Motaal, N.S. Mohamed, M.A. Tantawy, A. Belal, R. Alnajjar, W.M. Eldehna, A.A. Al-Karmalawy, Design and synthesis of novel benzoazoninone derivatives as potential CBSIs and apoptotic inducers: In Vitro, in Vivo, molecular docking, molecular dynamics, and SAR studies, Bioorg Chem, 127 (2022) 105995.
[16] H. Zhang, H.Z. Qi, J. Mao, H.R. Zhang, Q.Q. Luo, M.L. Hu, C. Shen, L. Ding, Discovery of novel microtubule stabilizers targeting taxane binding site by applying molecular docking, molecular dynamics simulation, and anticancer activity testing, Bioorg Chem, 122 (2022) 105722.
[17] D. Havrylyuk, O. Roman, R. Lesyk, Synthetic approaches, structure activity relationship and biological applications for pharmacologically attractive pyrazole/pyrazoline-thiazolidine-based hybrids, Eur J Med Chem, 113 (2016) 145-166.
[18] K.M. Qiu, R. Yan, M. Xing, H.H. Wang, H.E. Cui, H.B. Gong, H.L. Zhu, Synthesis, biological evaluation and molecular modeling of dihydro-pyrazolyl-thiazolinone derivatives as potential COX-2 inhibitors, Bioorg Med Chem, 20 (2012) 6648-6654.
[19] N.D. Amnerkar, K.P. Bhusari, Synthesis, anticonvulsant activity and 3D-QSAR study of some prop-2-eneamido and 1-acetyl-pyrazolin derivatives of aminobenzothiazole, Eur J Med Chem, 45 (2010) 149-159.
[20] P.-C. Lv, H.-Q. Li, J. Sun, Y. Zhou, H.-L. Zhu, Synthesis and biological evaluation of pyrazole derivatives containing thiourea skeleton as anticancer agents, Bioorganic & Medicinal Chemistry, 18 (2010) 4606-4614.
[21] S.S. El-Nakkady, M.M. Hanna, H.M. Roaiah, I.A. Ghannam, Synthesis, molecular docking study and antitumor activity of novel 2-phenylindole derivatives, Eur J Med Chem, 47 (2012) 387-398.
[22] M. Abdel-Aziz, O.M. Aly, S.S. Khan, K. Mukherjee, S. Bane, Synthesis, cytotoxic properties and tubulin polymerization inhibitory activity of novel 2-pyrazoline derivatives, Arch Pharm (Weinheim), 345 (2012) 535-548.
[23] C. Wang, S. Yang, J. Du, J. Ni, Y. Wu, J. Wang, Q. Guan, D. Zuo, K. Bao, Y. Wu, W. Zhang, Synthesis and bioevaluation of diarylpyrazoles as antiproliferative agents, Eur J Med Chem, 171 (2019) 1-10.
[24] P.C. Lv, D.D. Li, Q.S. Li, X. Lu, Z.P. Xiao, H.L. Zhu, Synthesis, molecular docking and evaluation of thiazolyl-pyrazoline derivatives as EGFR TK inhibitors and potential anticancer agents, Bioorg Med Chem Lett, 21 (2011) 5374-5377.
[25] R.F. George, M. Kandeel, D.Y. El-Ansary, A.M. El Kerdawy, Some 1,3,5-trisubstituted pyrazoline derivatives targeting breast cancer: Design, synthesis, cytotoxic activity, EGFR inhibition and molecular docking, Bioorg Chem, 99 (2020) 103780.
[26] M.S. Abdel-Maksoud, R. Mohamed Hassan, A. Abdel-Sattar El-Azzouny, M. Nabil Aboul-Enein, C.H. Oh, Anticancer profile and anti-inflammatory effect of new N-(2-((4-(1,3-diphenyl-1H-pyrazol-4-yl)pyridine sulfonamide derivatives, Bioorg Chem, 117 (2021) 105424.
[27] S.Y. Shin, H. Yoon, D. Hwang, S. Ahn, D.W. Kim, D. Koh, Y.H. Lee, Y. Lim, Benzochalcones bearing pyrazoline moieties show anti-colorectal cancer activities and selective inhibitory effects on aurora kinases, Bioorg Med Chem, 21 (2013) 7018-7024.
[28] M. Yu, H. Yang, K. Wu, Y. Ji, L. Ju, X. Lu, Novel pyrazoline derivatives as bi-inhibitor of COX-2 and B-Raf in treating cervical carcinoma, Bioorg Med Chem, 22 (2014) 4109-4118.
[29] K. Haider, M. Shafeeque, S. Yahya, M.S. Yar, A comprehensive review on pyrazoline based heterocyclic hybrids as potent anticancer agents, Eur J Med Chem Reports, 5 (2022) 100042.
[30] N. Hura, A. Naaz, S.S. Prassanawar, S.K. Guchhait, D. Panda, Drug-Clinical Agent Molecular Hybrid: Synthesis of Diaryl(trifluoromethyl)pyrazoles as Tubulin Targeting Anticancer Agents, ACS Omega, 3 (2018) 1955-1969.
[31] B. Yang, J. Zhou, F. Wang, X.-W. Hu, Y. Shi, Pyrazoline derivatives as tubulin polymerization inhibitors with one hit for Vascular Endothelial Growth Factor Receptor 2 inhibition, Bioorg Chem, 114 (2021) 105134.

[32] M. Hawash, S.G. Ergun, D.C. Kahraman, A. Olgac, E. Hamel, R. Cetin-Atalay, S.N. Baytas, Novel indole-pyrazole hybrids as potential tubulin-targeting agents; Synthesis, antiproliferative evaluation, and molecular modeling studies, J Mol Struct, 1285 (2023) 135477.
[33] D. Matiadis, M. Sagnou, Pyrazoline Hybrids as Promising Anticancer Agents: An Up-to-Date Overview, Int J Mol Sci, 21 (2020) 5507.
[34] Y.-L. Zhang, Y.-J. Qin, D.-J. Tang, M.-R. Yang, B.-Y. Li, Y.-T. Wang, H.-Y. Cai, B.-Z. Wang, H.-L. Zhu, Synthesis and Biological Evaluation of 1-Methyl-1H-indole–Pyrazoline Hybrids as Potential Tubulin Polymerization Inhibitors, ChemMedChem, 11 (2016) 1446-1458.
[35] A. Fan, Y. Zhang, Q. Zhang, J. Wei, X. Lu, G. Ren, D. Zhao, N. Li, H. Zhu, X. Chen, Evaluation of the pharmacokinetics, tissue distribution and excretion studies of YMR-65, a tubulin polymerization inhibitor with potential anticancer activity, in rats using UPLC-MS/MS, Xenobiotica, 48 (2018) 920-926.
[36] A. Fan, J. Wei, M. Yang, Q. Zhang, Y. Zhang, Q. Liu, N. Li, D. Zhao, Y. Lu, J. Li, J. Zhao, S. Deng, B. Zhang, H. Zhu, X. Chen, Pharmacodynamic and pharmacokinetic characteristics of YMR-65, a tubulin inhibitor, in tumor-bearing mice, Eur J Pharm Sci, 121 (2018) 74-84.
[37] K. Chen, Y.L. Zhang, J. Fan, X. Ma, Y.J. Qin, H.L. Zhu, Novel nicotinoyl pyrazoline derivates bearing N-methyl indole moiety as antitumor agents: Design, synthesis and evaluation, Eur J Med Chem, 156 (2018) 722-737.
[38] G. Li, J.-Q. Wu, X. Cai, W. Guan, Z. Zeng, Y. Ou, X. Wu, J. Li, X. Fang, J. Liu, Y. Zhang, H. Wang, C. Yin, H. Yao, Design, synthesis, and biological evaluation of diaryl heterocyclic derivatives targeting tubulin polymerization with potent anticancer activities, Eur J Med Chem, 252 (2023) 115284.
[39] H. Tallima, R. El Ridi, Mechanisms of Arachidonic Acid In Vitro Tumoricidal Impact, Molecules, 28 (2023) 1727.
[40] A. Sabt, M.A. Khedr, W.M. Eldehna, A.I. Elshamy, M.F. Abdelhameed, R.M. Allam, R.Z. Batran, New pyrazolylindolin-2-one based coumarin derivatives as anti-melanoma agents: design, synthesis, dual BRAFV600E/VEGFR-2 inhibition, and computational studies, RSC Advances, 14 (2024) 5907-5925.
[41] P. Skehan, R. Storeng, D. Scudiero, A. Monks, J. McMahon, D. Vistica, J.T. Warren, H. Bokesch, S. Kenney, M.R. Boyd, New colorimetric cytotoxicity assay for anticancer-drug screening, J Natl Cancer Inst, 82 (1990) 1107-1112.
[42] I.A.Y. Ghannam, H.M. Roaiah, M.M. Hanna, S.S. El-Nakkady, R.J. Cox, Identification, crystal structure and antitumor activity of fusaric acid from the sugarcane fungal pathogen, Fusarium sacchari, Int J Pharm Technol, 6 (2014) 6528–6535.
[43] I.H. Ali, H.T. Abdel-Mohsen, M.M. Mounier, M.T. Abo-elfadl, A.M. El Kerdawy, I.A.Y. Ghannam, Design, synthesis and anticancer activity of novel 2-arylbenzimidazole/2-thiopyrimidines and 2-thioquinazolin-4(3H)-ones conjugates as targeted RAF and VEGFR-2 kinases inhibitors, Bioorganic Chemistry, 126 (2022) 105883.
[44] I.A.Y. Ghannam, A.M. El Kerdawy, H.T. Abdel-Mohsen, Imidazo[4,5-b]phenazines as Dual Topoisomerase I/IIα Inhibitors: Design, Synthesis, Biological Evaluation and Molecular Docking, Egypt J Chem, 65 (2022) 1157-1174.
[45] I.A.Y. Ghannam, A.M. El Kerdawy, M.M. Mounier, M.T. Abo-elfadl, I.H. Ali, Novel 2-oxo-2-phenylethoxy and benzyloxy diaryl urea hybrids as VEGFR-2 inhibitors: Design, synthesis, and anticancer evaluation, Arch Pharm (Weinheim), 356 (2023) 2200341.
[46] R.M. Hassan, I.H. Ali, A.M. El Kerdawy, M.T. Abo-Elfadl, I.A.Y. Ghannam, Novel benzenesulfonamides as dual VEGFR2/FGFR1 inhibitors targeting breast cancer: Design, synthesis, anticancer activity and in silico studies, Bioorg Chem, 152 (2024) 107728.
[47] H.T. Abdel-Mohsen, A.M. Nageeb, I.A.Y. Ghannam, Diphenyl urea-benzylidene acetohydrazide hybrids as fibroblast growth factor receptor 1 inhibitors and anticancer agents, Drug Dev Res, 85 (2024) e22249.
[48] I.A.Y. Ghannam, A.M. El Kerdawy, M.M. Mounier, M.T. Abo-elfadl, H.T. Abdel-Mohsen, Discovery of novel diaryl urea-oxindole hybrids as BRAF kinase inhibitors targeting BRAF and KRAS mutant cancers, Bioorg Chem, 153 (2024) 107848.
[49] S. Pochampally, K.L. Hartman, R. Wang, J. Wang, M.-K. Yun, K. Parmar, H. Park, B. Meibohm, S.W. White, W. Li, D.D. Miller, Design, Synthesis, and Biological Evaluation of Pyrimidine Dihydroquinoxalinone Derivatives as Tubulin Colchicine Site-Binding Agents That Displayed Potent Anticancer Activity Both In Vitro and In Vivo, ACS Pharmacol Transl Sci, 6 (2023) 526-545.

[50] E.H. Kellogg, N.M.A. Hejab, S. Howes, P. Northcote, J.H. Miller, J.F. Díaz, K.H. Downing, E. Nogales, Insights into the Distinct Mechanisms of Action of Taxane and Non-Taxane Microtubule Stabilizers from Cryo-EM Structures, J Mol Biol, 429 (2017) 633-646.
[51] https://www.rcsb.org/.
[52] A. Daina, O. Michielin, V. Zoete, SwissADME: a free web tool to evaluate pharmacokinetics, drug-likeness and medicinal chemistry friendliness of small molecules, Sci Reports, 7 (2017) 42717.
[53] A. Daina, O. Michielin, V. Zoete, iLOGP: a simple, robust, and efficient description of n-octanol/water partition coefficient for drug design using the GB/SA approach, J Chem Inf Model, 54 (2014) 3284-3301.
[54] A. Daina, V. Zoete, A BOILED-Egg To Predict Gastrointestinal Absorption and Brain Penetration of Small Molecules, ChemMedChem, 11 (2016) 1117-1121.
[55] M.N. Aboul-Enein, A.A. El-Azzouny, Y.A. Maklad, M.A. Ismail, N.S.M. Ismail, R.M. Hassan, Design and synthesis of certain substituted cycloalkanecarboxamides structurally related to safinamide with anticonvulsant potential, Res Chem Intermed, 41 (2015) 3767-3791.
[56] R.M. Hassan, M.E. Aboutabl, M. Bozzi, M.F. El-Behairy, A.M. El Kerdawy, B. Sampaolese, C. Desiderio, F. Vincenzoni, F. Sciandra, I.A.Y. Ghannam, Discovery of 4-benzyloxy and 4-(2-phenylethoxy) chalcone fibrate hybrids as novel PPARalpha agonists with anti-hyperlipidemic and antioxidant activities: Design, synthesis and in vitro/in vivo biological evaluation, Bioorg Chem, 115 (2021) 105170.
[57] I.H. Ali, R.M. Hassan, A.M. El Kerdawy, M.T. Abo-Elfadl, H.M.I. Abdallah, F. Sciandra, I.A.Y. Ghannam, Novel thiazolidin-4-one benzenesulfonamide hybrids as PPARγ agonists: Design, synthesis and in vivo anti-diabetic evaluation, Eur J Med Chem, 269 (2024) 116279.
[58] P.A. Halim, R.A. Hassan, K.O. Mohamed, S.O. Hassanin, M.G. Khalil, A.M. Abdou, E.O. Osman, Synthesis and biological evaluation of halogenated phenoxychalcones and their corresponding pyrazolines as cytotoxic agents in human breast cancer, J Enzyme Inhib Med Chem, 37 (2022) 189-201.
[59] W. Akhtar, A. Marella, M.M. Alam, M.F. Khan, M. Akhtar, T. Anwer, F. Khan, M. Naematullah, F. Azam, M.A. Rizvi, M. Shaquiquzzaman, Design and synthesis of pyrazole–pyrazoline hybrids as cancer-associated selective COX-2 inhibitors, Arch Pharm (Weinheim), 354 (2021) 2000116.
[60] D.F. Veber, S.R. Johnson, H.Y. Cheng, B.R. Smith, K.W. Ward, K.D. Kopple, Molecular properties that influence the oral bioavailability of drug candidates, J Med Chem, 45 (2002) 2615-2623.
[61] J. Ali, P. Camilleri, M.B. Brown, A.J. Hutt, S.B. Kirton, Revisiting the General Solubility Equation: In Silico Prediction of Aqueous Solubility Incorporating the Effect of Topographical Polar Surface Area, J Chem Inf Model, 52 (2012) 420-428.
[62] Y.C. Martin, A Bioavailability Score, J Med Chem, 48 (2005) 3164-3170.
[63] J.B. Baell, G.A. Holloway, New Substructure Filters for Removal of Pan Assay Interference Compounds (PAINS) from Screening Libraries and for Their Exclusion in Bioassays, J Med Chem, 53 (2010) 2719-2740.